Available online at www.sciencedirect.com
ScienceDirect
Journal of Magnetic Resonance 186 (2007) 193–200
JMR Journal of Magnetic Resonance
www.elsevier.com/locate/jmr

P.E.HSQC: A simple experiment for simultaneous and sign-sensitive measurement of $(^1J_{CH} + D_{CH})$ and $(^2J_{HH} + D_{HH})$ couplings

Pavleta Tzvetkova [a,b], Svetlana Simova [b], Burkhard Luy [a,*]

[a] Department Chemie, Organische Chemie II, Technische Universität München, Lichtenbergstrasse 4, D-85747 Garching, Germany
[b] Institute of Organic Chemistry, Bulgarian Academy of Sciences, Sofia, Bulgaria

Received 15 December 2006; revised 9 February 2007
Available online 14 February 2007

Abstract

The angular information content of residual dipolar couplings between nuclei of fixed distance makes the accurate and sign-sensitive measurement of $(^1J_{CH} + D_{CH})$ and $(^2J_{HH} + D_{HH})$ couplings highly desirable. Experiments published so far are typically highly specialized for the effective measurement of a subset of couplings. The P.E.HSQC presented here, is an E.COSY based experiment which allows the simultaneous measurement of all heteronuclear and homonuclear couplings within CH, CH_2, and CH_3 groups in a single spectrum with the necessary precision and sign information. The simplicity of the approach and the absence of artefacts like phase distortions due to antiphase evolution make it ideally suited for coupling determination of organic molecules at natural abundance.

Keywords: P.E.COSY; RDCs; Partial alignment; HSQC; Coupling constants

1. Introduction

Since the introduction of residual dipolar couplings (RDCs) in biomolecular NMR spectroscopy there is a vast number of experiments available for measuring heteronuclear one-bond couplings based on various principle techniques [1–13]. Most of these experiments are designed for IS spin systems, but a number of methods are also specifically designed for the needs of I_2S [14–20] and I_3S spin systems [21–24]. Because of the fixed geometry and the large dipolar couplings expected in the latter spin systems, it seems advantageous to also be able to measure the ^{1}H, ^{1}H-couplings within the spin groups. But all pulse sequences capable to do so have in common that at least two if not more subspectra have to be acquired for the extraction of a complete set of couplings.

A detailed examination of spectra shows in addition that in most experiments homonuclear coupling evolution is not fully suppressed and slight phase distortions in the presence of larger ^{1}H, ^{1}H-couplings can be observed (see e.g., slices of spectra shown in [14,13]). Only the SPITZE-HSQC [19] with HEHAHA transfer steps avoids this homonuclear antiphase evolution due to isotropic mixing conditions present during transfer periods with the disadvantage of a very limited bandwidth. In principle, homonuclear antiphase evolution could also be compensated by the application of CPMG-type pulse trains with homonuclear isotropic mixing conditions during the INEPT-type transfer steps [25–29], but this approach is power consuming and the common ^{13}C-bandwidth of ≈130 ppm for ^{1}H, ^{13}C one-bond correlation experiments cannot be covered by conventional probeheads at high-field spectrometers.

Here, a single, very simple experiment based on the E.COSY-principle for the simultaneous measurement of heteronuclear and homonuclear couplings within IS, I_2S, and I_3S spin systems is presented. The experiment is derived from the P.E.COSY [30] by transferring the original idea to the heteronuclear case and uses the same principle as the heteronuclear E.COSY experiment discussed in [31]. The resulting cross peaks in I_2S and I_3S spin systems cover roughly the same area in the two-dimensional

* Corresponding author. Fax: +49 89 289 13210.
E-mail address: Burkhard.Luy@ch.tum.de (B. Luy).

1090-7807/$ - see front matter © 2007 Elsevier Inc. All rights reserved.
doi:10.1016/j.jmr.2007.02.009

spectrum as in a t_2-coupled HSQC but the tilt of the E.COSY patterns allows the determination of homonuclear ($^2J_{HH} + D_{HH}$) couplings with their signs relative to the corresponding heteronuclear one-bond couplings.

2. Theory

Shortly after the introduction of the E.COSY principle [32,33] the so-called P.E.COSY or β-COSY experiment for the sign-sensitive coupling measurement between three coupled spins was introduced [31,30]. Instead of the long phase cycling schemes used in most of the previous experiments, a simple β-pulse is applied for conversion of antiphase magnetization into single quantum terms with the well-known E.COSY pattern. A compromise between a good signal-to-noise ratio and a clean E.COSY type multiplet pattern for three coupled spins in a non-phase cycled experiments is achieved when $30° \leqslant \beta \leqslant 40°$ [30].

The P.E.COSY can, of course, easily be transferred to the heteronuclear case by simply applying identical pulses on both protons and the heteronucleus. However, since the aim of the experiment is the conversion of antiphase magnetization, the initial excitation might be extended by an INEPT-step, which causes cosine-modulated inphase signals in the indirect dimension that potentially allow the application of simple 180° pulse decoupling schemes. The corresponding experiment termed P.E.HSQC is shown in Fig. 1b with details of the pulse sequence in the caption. As it turns out, a heteronuclear E.COSY experiment is already discussed in [31] where the problem corresponds to an activation or deactivation of a single spin by the mixing pulse. In this case the flip angle for the E.COSY mixing pulse on the single spin 1/2 can have an arbitrary value, with a 90° pulse resulting in the highest possible signal intensity.

Although no coherence order selection or other removal of ^{12}C-bound proton magnetization is applied, in our hands this basic experiment resulted in spectra of high quality with very little artefacts. Nevertheless, a further improved version of the P.E.HSQC is given in Fig. 1c with two adiabatic pulse/gradient combinations for efficient removal of all coherences including ZQ-terms [34]. The first ZQ-suppression scheme in this context is simply applied to destroy all coherences from previous scans and therefore clean up the starting polarization. We found that this trick slightly reduces t_1-noise in cases where the relaxation delay between scans is chosen too short. The second ZQ-suppression scheme ensures pure absorption spectra by the efficient removal of all unwanted homonuclear and heteronuclear coherences before acquisition. It therefore remarkably improves the appearance of signal quality.

Finally, a further variant of the experiment is shown in Fig. 1d: Since the preparation scheme of the P.E.HSQC results in cosine-modulated inphase signals in the indirect dimension, the very large multiplet-patterns can be reduced in size by partial decoupling. By choosing the factor κ in the pulse sequence scheme of Fig. 1d, the splitting due to

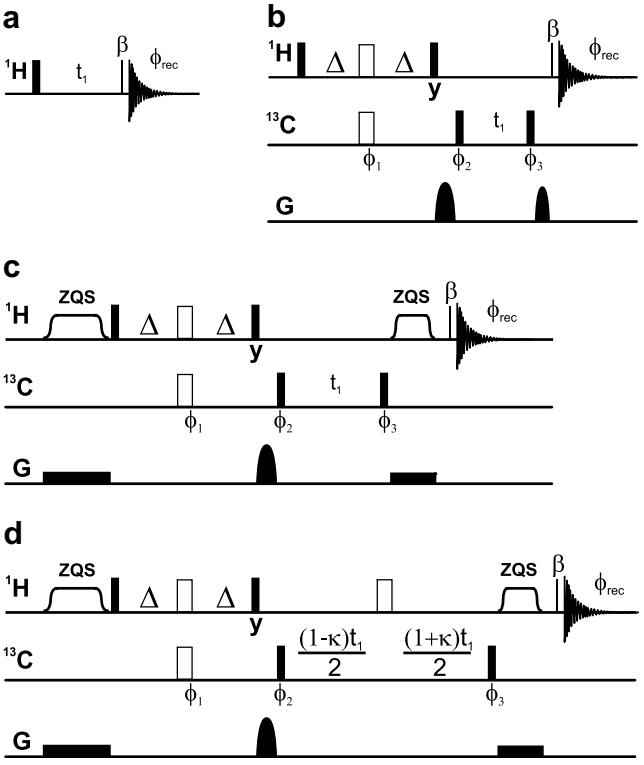

Fig. 1. Pulse sequences of the P.E.COSY and several versions of the proposed P.E.HSQC. (a) The original P.E.COSY as the starting point for the heteronuclear experiments introduced in this article, (b) the P.E.HSQC with purge gradients and additional versions with ZQ-suppression schemes for artefact reduction (c) and even partial decoupling during t_1 for improved multiplet appearance (d). All filled rectangles correspond to 90° pulses and open rectangles to 180° pulses along x unless specified otherwise. Thin bars annotated with β correspond to pulses with a flip angle of approximately 36° for the E.COSY-type multiplet patterns. Delays are set to $\Delta = 1/(4^1J_{CH})$ in all cases. Phase cycling was applied according to $\Phi_1 = 8(x), 8(-x)$, $\Phi_2 = x, -x$, $\Phi_3 = 4(x), 4(-x)$, and $\Phi_{rec} = x, -x, x, -x, -x, x, -x, x$. ZQ-suppression schemes were applied using 50 and 30 ms adiabatic CHIRP-pulses with simultaneous gradient pulses as described in [34]. κ indicates the scaling of the splitting in the indirect dimension: $\kappa = 1$ corresponds to full coupling evolution, $\kappa = 0$ to full decoupling, and $\kappa = 0.1$ leads to splittings that are scaled to 10% of the active coupling. Phase sensitive spectra are obtained in the States-TPPI or TPPI manner by phase cycling Φ_2 and Φ_{rec} accordingly.

coupling evolution of the $^1J_{CH}$ coupling is reduced to the same factor as demonstrated experimentally for $\kappa = 0.1$ in Figs. 3(c)–(c″) and 5.

The expected multiplet patterns of the P.E.HSQC for IS, I_2S, and I_3S spin systems are compared in Fig. 2 with conventional t_1- and t_2-coupled (a, a′, a″), and t_2-coupled HSQC experiments (b, b′, b″). For the simple IS case the multiplet is split by the $^1J_{CH}$ coupling in both dimensions and no additional information or multiplet reduction is gained (c). For the I_2S and I_3S spin systems, however, the resulting multiplet patterns of the P.E.HSQC show an E.COSY-type displacement that reveals the relative sign of ($^2J_{HH} + D_{HH}$) vs. ($^1J_{CH} + D_{CH}$) couplings and allows a simplified measurement of the homonuclear couplings (c′, c″).

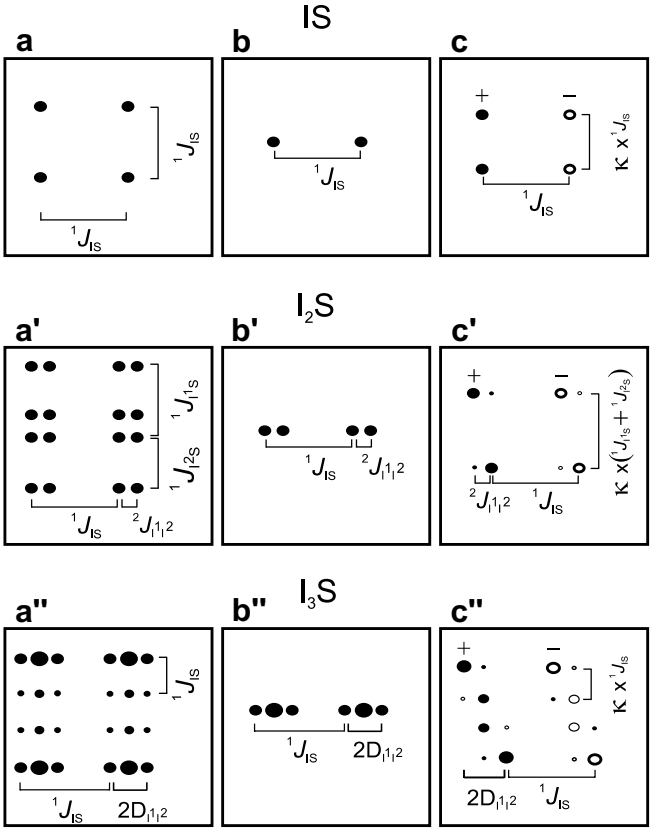

Fig. 2. Qualitative schematics for the expected multiplet patterns for IS, I_2S, and I_3S spin systems for a fully coupled HSQC (a), a t_1-decoupled, t_2-coupled HSQC (b), and the P.E.HSQC of Fig. 1b–d (c). Filled circles correspond to positive multiplet components, open circles to negative signals. Relative signal intensities are guided to the eye by the signal thickness. Scaling with κ refers to partial decoupling according to the sequence described in Fig. 1d. Homonuclear splittings within I_3S spin systems are only visible if samples are partially aligned and residual dipolar $D_{I_1I_2}$-couplings are present.

The relative multiplet intensities of the P.E.HSQC for the three different spin systems have been performed and evaluated by numerical simulations. For a fair comparison the relative intensities of IS, I_2S, and I_3S spin systems, resulting from a t_2-coupled HSQC, shall be examined first: the signal of a proton in the IS spin system splits in two, so that the maximum intensity of a multiplet component is equivalent to a normalized intensity of 0.5. In a I_2S spin system considering diastereotopic protons, the same amount of magnetization is split both by the heteronuclear and by the homonuclear scalar coupling, leading to a relative intensity of only 0.25 for the multiplet components. In methyl groups, three degenerate protons contribute to the signal, which, in partially aligned samples, leads to a doublet of triplets with an intensity of the strongest component of 0.75.

In contrast to the t_2-coupled HSQC, the P.E.HSQC in all cases has an additional splitting in the indirect dimension and therefore can be expected to have reduced multiplet intensities. For the I_2S spin system, nevertheless, the magnitude of the multiplet components is identical to the t_2-coupled HSQC with ≈0.25 per proton spin. The IS spin system results in four multiplet components, which again resembles an intensity of 0.25 per proton spin. The most complex multiplet, finally, is observed in dipolar coupled I_3S spin systems as qualitatively visualized in Fig. 2c″. The relative ratios of the four different multiplet component intensities taken from simulations are 0.27:0.16:−0.07:0.06 for a flip angle $\beta = 36°$. Most important for measuring $({}^1J_{CH} + D_{CH})$ and D_{HH} coupling constants are the outermost multiplet components with the highest signal intensity of 0.27. The signal intensities for the three different spin systems therefore are very similar and even can help reducing artifacts like t_1-noise from very intense methyl signals. In all cases the multiplets are at least as intense as the signal of an I_2S spin system in a t_2-coupled HSQC.

D_{HH} couplings in methyl groups generally contain the same structural information as the corresponding one-bond D_{CH} couplings. Since methyl groups rotate fast around the principle axis, which in most cases is along a C–C bond, all orientations are averaged except the angle α relative to this principal axis. For D_{CH} couplings, the interatomic vector describes an angle of $\alpha_{CH} = 109°$ and for D_{HH} couplings this angle is $\alpha_{HH} = 90°$. A geometrical scaling factor between these two vectors then is given by $s_{geo} = (3\cos^2\alpha_{HH} - 1)/(3\cos^2\alpha_{CH} - 1) = 3/2$ [35]. In addition, the size of dipolar couplings depends on the inverse cube of the interatomic distance and the participating gyromagnetic ratios. D_{HH} and D_{CH} couplings are therefore proportional with a constant scaling factor $D_{HH} = s_{geo}\gamma_H r_{CH}^3/(\gamma_C r_{HH}^3)D_{CH}$. A comparison of the strong dipolar coupling limit in the homonuclear case ($\mathcal{H}^{dip}_{I_1I_2} = 2\pi D_{I_1I_2}(2I_{1z}I_{2z} - I_{1x}I_{2x} - I_{1y}I_{2y}) = 2\pi D_{I_1I_2}(3I_{1z}I_{2z} - \mathbf{I_1I_2})$) versus the weak dipolar Hamiltonian ($\mathcal{H}^{dip}_{IS} = 2\pi D_{IS}(2I_zS_z)$) for the heteronuclear coupling leads to an additional scaling of the observed splitting of $s_{Ham} = 3/2$ [35]. With $\gamma_H/\gamma_C \approx 4$, $r_{CH} = 1.08$, and $r_{HH} = 1.76$, theory predicts a 2.08 times larger splitting for homonuclear compared to heteronuclear methyl RDCs, which closely resembles the experimentally derived factor 2.3 [36]. Altogether three pairs of D_{CH} and D_{HH} couplings in methyl groups have been measured for the ethyl ester (Fig. 5) which fulfill the theoretically predicted ratio within the error of measurement (Table 1). With the relative sign of $({}^1J_{CH} + D_{CH})$ and D_{HH} in methyl groups as obtained in the P.E.HSQC, unambiguous and accurate determination of dipolar couplings can be achieved even if very strong alignment would result in $D_{CH} > {}^1J_{CH}$ and therefore negative $({}^1J_{CH} + D_{CH})$ values.

3. Experimental

Altogether five samples were used in the studies presented. The three isotropic samples were dissolved in $CDCl_3$ (strychnine, ethyl ester) and DMSO-d_6 (pentapeptide). For the strychnine sample the solvent was purified with Al_2O_3 to remove any residual acid. Sample concentra-

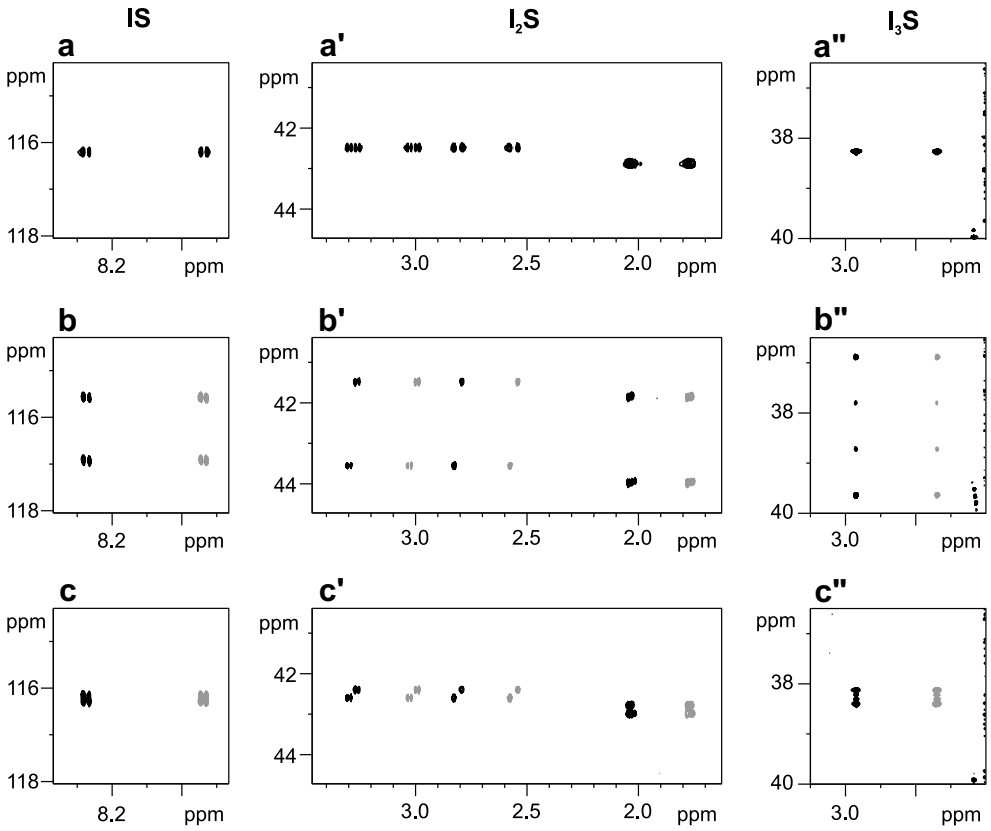

Fig. 3. Experimental multiplet patterns for IS, I_2S, and I_3S spin systems for a t_1-decoupled, t_2-coupled HSQC (a), a fully coupled P.E.HSQC (b) and a P.E.HSQC with partial decoupling according to $\kappa = 0.1$ (c). IS and I_2S spin systems are recorded on a strychnine sample dissolved in $CDCl_3$ and the I_3S spin system on a cyclic pentapeptide with N-methylation (see text for details). Grey signals correspond to negative contour levels. While the E.COSY-type pattern of the left and central I_2S spin system can nicely be seen, strong coupling leads to the removal of E.COSY displacements in the overlapped right most I_2S multiplet.

tions have been ≈35 mM for the pentapeptide cyclo-(D-Ala-Ala–N-Me–Ala-Ala-Ala), 100 mM for strychnine, and 150 mM for the ethyl ester of 5-dimethylphosphinyl-4-phenyl-2-(4-chlorophenyl)-2,3,4,5-tetrahydropyrrol-3-carboxylic acid (see [37] for synthesis and characterization). Two further samples were prepared in so-called alignment media, i.e. in a stretched poly(dimethylsiloxane) gel (PDMS-gel) and the liquid crystalline phase of poly(γ-benzyl-L-glutamate) (PBLG). The crosslinked PDMS gel as a member of polymer gel-based alignment media for organic solvents with arbitrarily scalable alignment [38–41] was prepared in house using the procedure described in [42,43]. For the gel with a deuterium splitting of $CDCl_3$ of 37 Hz we used a dry PDMS stick of 3 mm diameter and an accelerated electron irradiation dose of 200 kGy. The concentration of ethyl ester put on top of the already swollen gel corresponds to 150 mM, resulting in an estimated concentration inside the gel of ≈90 mM. For PBLG we followed the lengthy procedure described in [44–47] to obtain a sample with a final concentration of ≈300 mM and a deuterium splitting of 495 Hz (Fig. 4).

Most spectra were recorded on a Bruker AV500 spectrometer equipped with a 8 mm diameter probehead operating at 499.977 MHz for protons and 125.739 MHz for ^{13}C. The spectra of the ethyl ester inside the PDMS gel and the spectra of the pentapeptide in DMSO were recorded on a Bruker DMX600 spectrometer equipped with a 5 mm TXI inverse-detected probehead operating at 600.132 MHz for protons and 150.907 MHz for ^{13}C. No spinning was applied and temperature was controlled in all cases by Bruker BVT2000 or BVT3000 temperature units to be 298 °K. Spectra on partially aligned samples were acquired without lock on the solvent. Spectra for all samples were obtained using either the pulse programs shown in Fig. 1b–d or a Bruker standard HSQC without t_2-decoupling. Only HSQC data and data acquired with the sequence of Fig. 1c and d with $\kappa = 0.1$ are presented in this article. In all cases spectra were recorded with spectral digitization of 1024 (t_1) and 8192 (t_2) data points. The spectral widths for protons and ^{13}C varied from sample to sample and were as follows: for the strychnine sample 5252.1 Hz (^1H), 15087.4 Hz (^{13}C); for the pentapeptide sample 3004.8 Hz (^1H), 10058.2 Hz (^{13}C); for the unaligned ethyl ester sample 5252.1 Hz (^1H), 10057.7 Hz (^{13}C); for the ethyl ester in PBLG: 5252.1 Hz (^1H), 10058.2 Hz (^{13}C) and for the ethyl ester in PDMS 7183.9 Hz (^1H), 12072.7 Hz (^{13}C). The T_1-relaxation delay for all recorded spectra was set to 1 s. Spectra were processed using Bruker Topspin version 1.3 under Linux. All

Table 1
Couplings measured from spectral regions shown in Fig. 5

Spin system[a]	Coupling type	$\delta^{iso}(^1H)$ (ppm)[b]	Couplings in $CDCl_3$ (Hz)	Couplings in PDMS/$CDCl_3$ (Hz)	Couplings in PBLG/$CDCl_3$ (Hz)
IS (a)	$^1J_{CH} + D_{CH}$	3.44	136.1 ± 1.6	139.7 ± 0.8	262.6 ± 10.0
I_2S (b)	$^1J_{CH_1} + D_{CH_1}$	3.51	147.7 ± 0.8	148.4 ± 1.3	197.2 ± 2.0
	$^1J_{CH_2} + D_{CH_2}$	3.62	147.7 ± 0.8	148.7 ± 2.0	202.2 ± 2.0
	$^1J_{H_1H_2} + D_{H_1H_2}$	3.51/3.62	-10.6 ± 0.8	-9.8 ± 1.3	15.8 ± 3.0
I_3S (c)	$^1J_{CH} + D_{CH}$	0.70	127.8 ± 0.8	127.6 ± 0.8	145.3 ± 3.0
	D_{HH}	0.70		-0.8 ± 0.8	40.0 ± 3.0
I_3S (d)	$^1J_{CH} + D_{CH}$	1.20	128.1 ± 0.8	127.8 ± 0.8	119.1 ± 2.0
	D_{HH}	1.20		-0.9 ± 0.8	-19.1 ± 3.0
	$^1J_{PH} + D_{PH}$	1.20	-12.7 ± 0.8	-12.5 ± 1.3	-8.8 ± 3.0
	$^1J_{CP} + D_{CP}$	1.20	66.4 ± 5.0	67.1 ± 5.0	73.5 ± 5.0
I_3S (e)	$^1J_{CH} + D_{CH}$	1.43	128.2 ± 0.8	126.5 ± 0.8	101.5 ± 3.0
	D_{HH}	1.43		-4.4 ± 0.8	-60.0 ± 3.0
	$^1J_{PH} + D_{PH}$	1.43	-12.7 ± 0.8	-12.2 ± 1.3	-3.8 ± 3.0
	$^1J_{CP} + D_{CP}$	1.43	68.5 ± 5.0	69.1 ± 5.0	79.4 ± 5.0

[a] Letters in parentheses indicate annotation of the spin systems in Fig. 4.
[b] Chemical shifts are for the isotropic sample in $CDCl_3$. In alignment media chemical shifts change slightly.

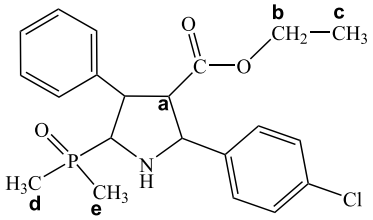

Fig. 4. Ethyl ester of 5-dimethylphosphinyl-4-phenyl-2-(4-chlorophenyl)-2,3,4,5-tetrahydropyrrol-3-carboxylic acid used for experiments in Fig. 5. Letters indicate spin systems for which couplings are reported in Table 1.

dimensions were apodized with 90° shifted quadratic sine bell functions and in spectra shown in Fig. 5 linear prediction has been applied. Matrices were zero filled to 2k points in the indirect dimension before Fourier transform. The spectrum shown in Fig. 6 was acquired using offset and rf-amplitude compensated BEBOP and BIBOP pulses taken from [52] with 337.5 and 307.5 μs duration for the carbon channel. The pulses cover a bandwidth of 20 kHz and can tolerate B_1-field inhomogeneities up to ±20%. BEBOP and time-reversed BEBOP pulses for transfers according to $2I_zS_z \rightarrow 2I_zS_y$ and $2I_zS_y \rightarrow 2I_zS_z$ are applied as described in [48].

4. Discussion

The introduced P.E.HSQC has several advantages and disadvantages compared to previously published experiments. The main disadvantage is certainly the detected antiphase magnetization which does not allow heteronuclear decoupling schemes to be applied. The experiment therefore leads to split signals in the direct detected dimension and has its major application in the measurement of coupling constants in contrast to heteronuclear decoupled HSQC and HMQC based methods. The signal-to-noise ratio of the P.E.HSQC has been compared in detail with a t_1-decoupled, t_2-coupled HSQC experiments without sensitivity enhancement. Although generally signal intensities are reduced in the P.E.HSQC, it is equivalent for methylene groups as the least intense signals. Sensitivity enhanced HSQC experiments considering matched delays optimized for methylene spin systems theoretically should give a $\sqrt{2}$ better sensitivity. The P.E.HSQC is also not optimized in terms of resolution, as a number of experimental schemes are available that provide separated multiplet components in a number of subspectra [19,13] that seem to be more appropriate for larger molecules with significant overlap.

The main advantage of the P.E.HSQC is the simplicity of its approach. The setup of the experiment is very straightforward with very low power consumption and without limitation with respect to bandwidth as for the SPITZE-HSQC [19]. Two novel uses of the ZQ-suppression scheme are introduced that lead to reduced t_1-noise and pure absorptive detection. The resulting spectra do show very little artefacts and can be interpreted very easily. Phase distortions due to homonuclear couplings as observed for some HSQC variants are not present in the P.E.HSQC.

Usually heteronuclear correlation experiments do not take into account strong coupling artefacts and the P.E.HSQC is no exception. As is shown in Fig. 3a′–c′ for the righthand signal, second order effects severely distort the E.COSY pattern of the P.E.HSQC. The two protons of the methylene group with chemical shifts only a few Hz apart interchange α and β states in both t_1 and t_2 evolution periods due to the strong coupling condition and the required condition of conserved spin states for the E.COSY displacement cannot be met. In such a case, couplings cannot reliably be measured without fitting the complete multiplet structure including all coupled spins.

A problem for conventional HSQC experiments measured on partially oriented samples is the wide distribution

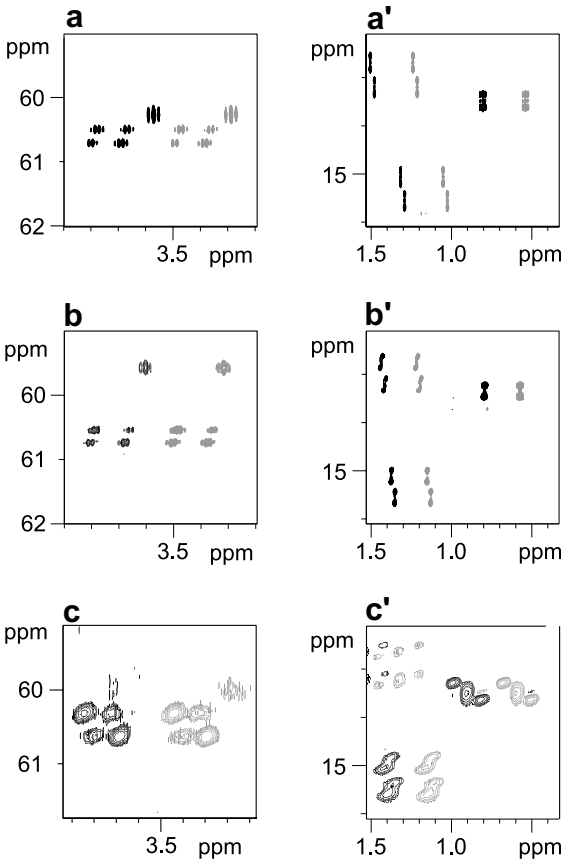

Fig. 5. Measurement of ($^1J_{CH} + D_{CH}$) and ($^2J_{HH} + D_{HH}$) couplings of an ethyl ester (Fig. 4) in $CDCl_3$ (a, a′), aligned in a stretched PDMS/$CDCl_3$ gel (b, b′), and aligned in PBLG/$CDCl_3$ (c, c′) using the pulse sequence shown in Fig. 1d. Clearly the E.COSY-patterns are visible for the unaligned and aligned CH_2 group and the three aligned CH_3 groups. A right tilt as visible in (a) for the CH_2-group corresponds to a negative ^{1}H, ^{1}H-coupling relative to the scaled ^{13}C, ^{1}H-coupling in the indirect dimension. Two of the methyl groups are additionally split by ^{1}H–^{31}P and ^{13}C–^{31}P couplings. It should be noted that sign reversal takes place for the ^{1}H, ^{1}H-coupling of the methylene group upon alignment in PBLG. This would most likely be left undetected and maybe even misinterpreted in conventional coupled HSQC-spectra.

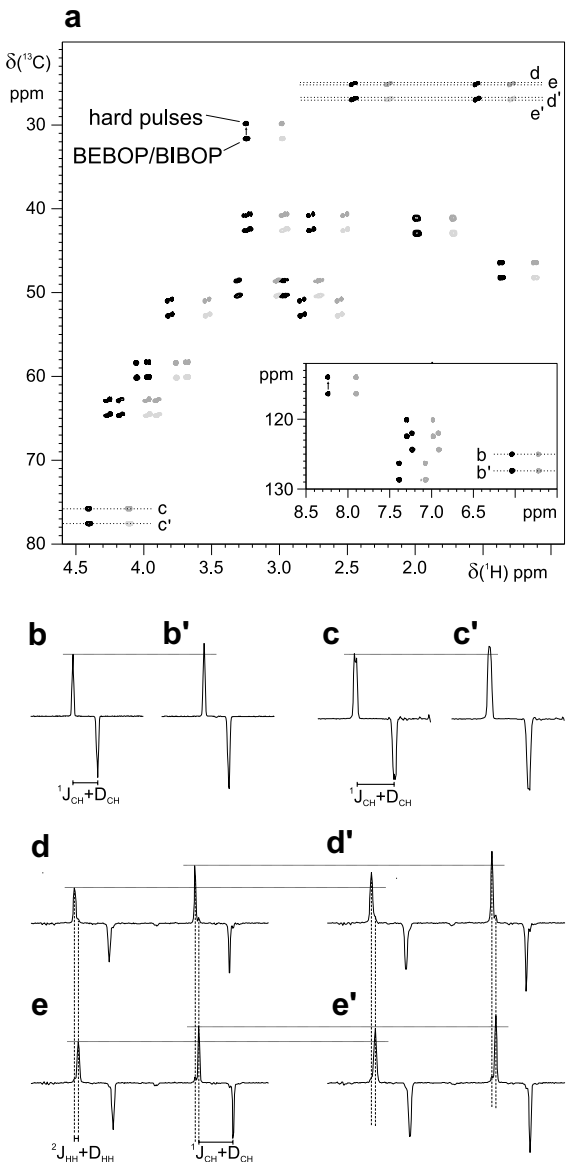

Fig. 6. Comparison of the P.E.HSQC experiment acquired on strychnine with standard ^{13}C hard pulses and BEBOP and BIBOP shaped pulses as previously described for HSQC and HMBC experiments [48]. (a) Contour plot of the BEBOP/BIBOP experiment and the hard pulse experiment shifted in the carbon dimension for better comparison. The inlet shows the aromatic region. Dotted lines and corresponding letters indicate slices drawn underneath. Simple letters represent slices through hard pulse cross peaks while slices through BEBOP/BIBOP cross peaks are marked with a prime. Slices for the aromatic (b, b′), central (c, c′) and far aliphatic (d, d′, e, e′) regions are chosen to cover the whole offset range. Improvements in signal to noise due to the application of shaped pulses are visualized by horizontal lines. For the CH_2 group shown in (d,d′,e,e′) dashed lines guide the sign-sensitive measurement of ($^2J_{HH} + D_{HH}$) couplings using the E.COSY-type displacement.

of heteronuclear one-bond couplings. Resulting phase distortions and signal losses due to imperfectly matched delays increase strongly with the duration of transfer periods. Here, again, the P.E.HSQC has a significant advantage over other HSQC-based schemes since only a single INEPT step is needed for preparation and no delay for the back-transfer needs to be matched which otherwise could lead to substantial losses in signal intensity.

Hard pulses usually do not equally cover the full ^{13}C-chemical shift range [48]. For even further improved pulse sequence performance optimized broadband pulses can be implemented, as for example the optimal control derived BEBOP and BIBOP pulses with excellent offset behavior and B_1-field compensation [48–53]. An experimental comparison of a standard hard pulse vs. a BEBOP/BIBOP pulse version of the P.E.HSQC is given in Fig. 6. For all cross peaks a significant improvement in terms of signal-to-noise can be observed, leading to an ≈12% increased sensitivity onresonant and up to a 35% increase at the edges of the carbon chemical shift range.

For the case that no gradients are available, experiments can be modified by introducing well-known ^{13}C-filtering schemes like the BIRD-element [54], spin-lock purge pulses [55] or simultaneous application of both schemes [56,57].

Very good performance of the P.E.HSQC has been achieved without gradients (spectra not shown) by the simultaneous application of a BIRD element and two spin-lock purge pulses with only slightly increased t_1-noise due to residual ^{12}C-bound magnetization.

5. Conclusion

The P.E.HSQC is introduced as a single, easy to apply experiment for simultaneous, sign-sensitive measurement of $(^1J_{CH} + D_{CH})$ and $(^2J_{HH} + D_{HH})$ couplings. Similar to the well-known P.E.COSY for homonuclear correlations, the final mixing step in the heteronuclear correlation experiment is achieved by a β-pulse. Additional features for cleaning the spectra and scaling of the splittings due to large $(^1J_{CH} + D_{CH})$ coupling in the indirect dimension are proposed. Due to the E.COSY pattern additional information regarding sign and size of homonuclear couplings within the spin systems is gained in comparison to t_1-decoupled, t_2-coupled HSQC experiments, while retaining roughly the same signal area for I_2S and I_3S groups. The spectral quality of the P.E.HSQC is very good with practically no phase distortions. The P.E.HSQC might well be expected to become a standard experiment for measuring $(^1J_{CH} + D_{CH})$ and the corresponding $(^2J_{HH} + D_{HH})$ couplings in small to medium-sized molecules.

Acknowledgments

B.L. thanks the Fonds der Chemischen Industrie and the DFG for financial support (Emmy Noether fellowship LU 835/1).

References

[1] M.D. Sørensen, A. Meissner, O.W. Sørensen, Spin-state-selective coherence transfer via intermediate states of two-spin coherence in IS spin systems. Application to E.COSY-type measurement of J coupling constants, J. Biomol. NMR 10 (1997) 181–186.

[2] A. Meissner, J.O. Duus, O.W. Sørensen, Integration of spin-state selective excitation into 2D NMR correlation experiments with heteronuclear ZQ/DQ π rotations for $^1J_{XH}$-resolved E.COSY-type measurement of heteronuclear coupling constants in proteins, J. Biomol. NMR 10 (1997) 89–94.

[3] P. Andersson, J. Weigelt, G. Otting, Spin-state selection filters for the measurement of heteronuclear one-bond coupling constants, J. Biomol. NMR 12 (1998) 435–441.

[4] M.D. Sørensen, A. Meissner, O.W. Sørensen, ^{13}C natural abundance S^3E and S^3CT experiments for measurement of J coupling constants between ^{13}Cα or ^{1}Hα and other protons in a protein, J. Magn. Reson. 137 (1999) 237–242.

[5] M. Ottiger, F. Delaglio, A. Bax, Measurement of J and dipolar couplings from simplified two-dimensional NMR spectra, J. Magn. Reson. 131 (1998) 373–378.

[6] T. Parella, M. Gairí, Simultaneous recording of spin-state-selective NMR spectra for different I_nS spin systems, J. Am. Chem. Soc. 126 (2004) 9821–9826.

[7] P. Permi, A spin-state-selective experiment for measuring heteronuclear one-bond and homonuclear two-bond couplings from an HSQC-type spectrum, J. Biomol. NMR 22 (2002) 27–35.

[8] P. Permi, Two simple NMR experiments for measuring dipolar couplings in asparagines and glutamine side chains, J. Magn. Reson. 153 (2001) 267–272.

[9] K. Ding, A.M. Gronenborn, Sensitivity-enhanced E.COSY-type HSQC experiments for accurate measurements of one-bond ^{15}N–^{1}HN, ^{15}N–^{13}CO and two-bond ^{13}CO–^{1}HN residual couplings in proteins, J. Magn. Reson. 158 (2002) 173–177.

[10] B. Luy, J.J. Barchi, J.P. Marino, S^3E-E.COSY methods for the measurement of ^{19}F associated scalar and dipolar coupling constants, J. Magn. Reson. 152 (2001) 179–184.

[11] B. Luy, J.P. Marino, Measurement and application of ^{1}H–^{19}F dipolar couplings in the structure determination of 2′-fluorolabeled RNA, J. Biomol. NMR 20 (2001) 39–47.

[12] B. Luy, J.P. Marino, JE-TROSY: Combined J- and TROSY-Spectroscopy for the measurement of one bond couplings in macromolecules, J. Magn. Reson. 163 (2003) 92–98.

[13] P. Nolis, J.F. Espinosa, T. Parella, Optimum spin-state selection for all multiplicities in the acquisition dimension of the HSQC experiment, J. Magn. Reson. 180 (2006) 39–50.

[14] M. Sattler, J. Schleucher, O. Schedletzky, S.J. Glaser, C. Griesinger, N.C. Nielsen, O.W. Sørensen, α&β HSQC, an HSQC-type experiment with improved resolution for I_2S groups, J. Magn. Reson. A 119 (1996) 171–179.

[15] T.S. Untidt, T. Schulte-Herbrüggen, O.W. Sørensen, N.C. Nielsen, Nuclear Magnetic Resonance coherence-order and spin-state-selective correlation in I_2S spin systems, J. Phys. Chem. A 103 (1999) 8921–8926.

[16] E. Miclet, E. O'Neil-Cabello, E.P. Nikonowicz, D. Live, A. Bax, ^{1}H–^{1}H dipolar couplings provide a unique probe of RNA backbone structure, J. Am. Chem. Soc. 125 (2003) 15740–15741.

[17] E. Miclet, J. Boisbouvier, A. Bax, Measurement of eight scalar and dipolar couplings for methine–methylene pairs in proteins and nucleic acids, J. Biomol. NMR 31 (2005) 201–216.

[18] E. Miclet, D.C. Williams Jr., G.M. Clore, D.L. Bryce, J. Boisbouvier, A. Bax, Relaxation-optimized NMR spectroscopy of methylene groups in proteins and nucleic acids, J. Am. Chem. Soc. 126 (2004) 10560–10570.

[19] T. Carlomagno, W. Peti, C. Griesinger, A new method for the simultaneous measurement of magnitude and sign of $^1D_{CH}$ and $^1D_{HH}$ dipolar couplings in methylene groups, J. Biomol. NMR 17 (2000) 99–109.

[20] K. Fehér, K. Kövér, Measurement of one-bond heteronuclear dipolar coupling contributions for amine and diastereotopic methylene protons, J. Magn. Reson. 168 (2004) 307–313.

[21] V. Tugarinov, P.M. Hwang, J.E. Ollerenshaw, L.E. Kay, Crosscorrelated relaxation enhanced ^{1}H–^{13}C NMR spectroscopy of methyl groups in very high molecular weight proteins and protein complexes, J. Am. Chem. Soc. 125 (2003) 10420–10428.

[22] J.E. Ollerenshaw, V. Tugarinov, L.E. Kay, Methyl TROSY: explanation and experimental verification, Magn. Reson. Chem. 41 (2003) 843–862.

[23] G. Kontaxis, A. Bax, Multiplet component separation for measurement of methyl ^{13}C–^{1}H dipolar couplings in weakly aligned proteins, J. Biomol. NMR 20 (2001) 77–82.

[24] K. Pervushin, B. Vögeli, Observation of individual transitions in magnetically equivalent spin systems, J. Am. Chem. Soc. 125 (2003) 9566–9567.

[25] B. Luy, J.P. Marino, ^{1}H–^{31}P CPMG-correlated experiments for the assignment of nucleic acids, J. Am. Chem. Soc. 123 (2001) 11306–11307.

[26] H. Koskela, I. Kilpelainen, S. Heikkinen, LR-CAHSQC: an application of a Carr-Purcell-Meiboom-Gill-type sequence to heteronuclear multiple bond correlation spectroscopy, J. Magn. Reson. 164 (2003) 228–232.

[27] K.E. Kövér, G. Batta, K. Fehér, Accurate measurement of long-range heteronuclear coupling constants from undistorted multiplets of an enhanced CPMG-HSQMBC experiment, J. Magn. Reson. 181 (2006) 89–97.

[28] V. Lacerda, G.V.J. da Silva, M.G. Constantino, C.F. Tormena, R.T. Williamson, B.L. Marquez, Long-range J_{CH} heteronuclear coupling constants in cyclopentane derivatives, Magn. Reson. Chem. 44 (2006) 95–98.
[29] H. Koskela, I. Kilpelainen, S. Heikkinen, CAGEBIRD: improving the GBIRD filter with a CPMG sequence, J. Magn. Reson. 170 (2004) 121–126.
[30] L. Mueller, P.E. COSY, A simple alternative to E.COSY, J. Magn. Reson. 72 (1987) 191–196.
[31] C. Griesinger, O.W. Sørensen, R.R. Ernst, Correlation of connected transitions by two-dimensional NMR spectroscopy, J. Chem. Phys. 85 (1986) 6837–6852.
[32] C. Griesinger, O.W. Sørensen, R.R. Ernst, Two-dimensional correlation of connected NMR transitions, J. Am. Chem. Soc. 107 (1985) 6394–6396.
[33] C. Griesinger, O.W. Sørensen, R.R. Ernst, Practical aspects of the E.COSY technique. Measurement of scalar spin–spin coupling constants in peptides, J. Magn. Reson. 75 (1987) 474–492.
[34] M.J. Thrippleton, J. Keeler, Elimination of zero-quantum interference in two-dimensional NMR spectra, Angew. Chem. Int. Ed. 42 (2003) 3938–3941.
[35] J.W. Emsley, J.C. Lindon, NMR spectroscopy using liquid crystal solvents, Pergamon Press, Aylesbury, 1975.
[36] A. Kaikkonen, G. Otting, Residual dipolar ^{1}H–^{1}H couplings of methyl groups in weakly aligned proteins, J. Am. Chem. Soc. 123 (2001) 1770–1771.
[37] Tsv. Cholakova, Y. Zagraniarsky, S. Simova, S. Varbanov, A. Dobrev, A simple synthesis of dimethylphosphinyl-substituted tetrahydropyrroles, Phosphorus Sulfur and Silicon 180 (2005) 1721–1728.
[38] B. Luy, K. Kobzar, H. Kessler, Easy and scalable method for the partial alignment of organic molecules for measuring residual dipolar couplings, Angew. Chem. Int. Ed. 43 (2004) 1092–1094.
[39] B. Luy, K. Kobzar, S. Knör, D. Heckmann, J. Furrer, H. Kessler, Orientational properties of stretched poly(styrene) gels in various organic solvents and the suppression of its residual ^{1}H NMR signals, J. Am. Chem. Soc. 127 (2005) 6459–6465.
[40] J.C. Freudenberger, S. Knör, K. Kobzar, D. Heckmann, T. Paululat, H. Kessler, B. Luy, Stretched polyvinylacetate-gels as NMR-alignment media for the measurement of residual dipolar couplings in polar organic solvents, Angew. Chem. Int. Ed. 44 (2005) 423–426.
[41] P. Haberz, J. Farjon, C. Griesinger, A DMSO-compatible orienting medium: towards the investigation of the stereochemistry of natural products, Angew. Chem. Int. Ed. 44 (2005) 427–429.
[42] J.C. Freudenberger, P. Spiteller, R. Bauer, H. Kessler, B. Luy, Stretched polydimethylsiloxane gels as nmr-alignment media for apolar and weakly polar organic solvents: ideal tool for measuring RDCs at low molecular concentrations, J. Am. Chem. Soc. 126 (2004) 14690–14691.
[43] J. Klages, C. Neubauer, M. Coles, H. Kessler, B. Luy, Structure refinement of Cyclosporin A in chloroform using RDCs measured in a stretched PDMS-gel, ChemBioChem 6 (2005) 1672–1678.
[44] P. Lesot, D. Merlet, A. Loewenstein, J. Courtieu, Enantiomeric visualization using proton-decoupled natural abundance deuterium NMR in poly(γ-benzyl-L-glutamate) liquid crystalline solutions, Tetrahedron: Asymmetry 9 (1998) 1871–1881.
[45] D. Merlet, B. Ancian, J. Courtieu, P. Lesot, Two-dimensional deuterium NMR spectroscopy of chiral molecules oriented in a polypeptide liquid crystal: applications for the enantiomeric analysis through natural abundance deuterium NMR, J. Am. Chem. Soc. 121 (1999) 5249–5258.
[46] M. Sarfati, J. Courtieu, P. Lesot, First successful enantiomeric discrimination of chiral alkanes using NMR spectroscopy, Chem. Commun. 13 (2000) 1113–1114.
[47] C.M. Thiele, S. Berger, Probing the diastereotopicity of methylene protons in strychnine using residual dipolar couplings, Org. Lett. 5 (2003) 705–708.
[48] T.E. Skinner, K. Kobzar, B. Luy, R. Bendall, W. Bermel, N. Khaneja, S.J. Glaser, Optimal control design of constant amplitude phase-modulated pulses: application to calibration-free broadband excitation, J. Magn. Reson. 179 (2006) 241–249.
[49] T. Skinner, T. Reiss, B. Luy, N. Khaneja, S.J. Glaser, Application of Optimal Control Theory to the design of broadband excitation pulses for high resolution NMR, J. Magn. Reson. 163 (2003) 8–15.
[50] T.E. Skinner, T.O. Reiss, B. Luy, N. Khaneja, S.J. Glaser, Reducing the duration of broadband excitation pulses using optimal control with limited RF amplitude, J. Magn. Reson. 167 (2004) 68–74.
[51] T. Skinner, T.O. Reiss, B. Luy, N. Khaneja, S.J. Glaser, Tailoring the optimal control cost function to enable shorter broadband excitation pulses, J. Magn. Reson. 172 (2005) 17–23.
[52] K. Kobzar, T. Skinner, N. Khaneja, S.J. Glaser, B. Luy, Exploring the limits of broadband excitation and inversion pulses, J. Magn. Reson. 170 (2004) 236–243.
[53] B. Luy, K. Kobzar, T.E. Skinner, N. Khaneja, S.J. Glaser, Construction of universal rotations from point to point transformations, J. Magn. Reson. 176 (2005) 179–186.
[54] J.R. Garbow, D.P. Weitekamp, A. Pines, Bilinear rotation decoupling of homonuclear scalar interactions, Chem. Phys. Lett. 93 (1982) 504–509.
[55] G. Otting, K. Wüthrich, Efficient purging scheme for proton-detected heteronuclear two-dimensional NMR, J. Magn. Reson. 76 (1988) 569–574.
[56] J.M. Nuzillard, G. Gasmi, J.M. Bernassau, HMQC experiment with single scan per t_1 value and without field gradient pulses, J. Magn. Reson. A 104 (1993) 83–87.
[57] S. Simova, Application of HSQC to the measurement of homonuclear coupling constants $J(H,H)$, Magn. Reson. Chem. 36 (1998) 505–510.